

# Raman spectra of the materials based on mechanically activated alkaline earth metal titanates

Vera P. Pavlović, Ani Tshantshapanyan, Branislav Vlahović,  
Jelena Živojinović, Darko Kosanović, Vladimir B. Pavlović

**Abstract** — The changes in the Raman spectra of electronic materials obtained from mechanically activated BaTiO<sub>3</sub> and SrTiO<sub>3</sub> powders, with or without additives, are presented in this paper. Mechanical activation, performed in a high-energy planetary ball mill, was chosen as the method for the production of fine-grained nanocrystalline powders with an increased surface activity and an altered micro and/or crystal structure. Having in mind the growing relevance of the development of multiferroic materials, the analysis of Raman spectra was used not only for the structural investigations of the mechanically activated undoped titanate powder, but also for the examination of the mechanically activated Fe/BaTiO<sub>3</sub> system and the subsequent hexaferrite formation during the sintering process. Additionally, Raman spectroscopy was applied in the study of the emergence of electroactive crystalline phases in nanocomposites based on semi-crystalline fluoropolymers, such as PVDF (polyvinylidene fluoride), in the case when mechanically activated BaTiO<sub>3</sub> powder was used as a filler in the polymer matrix. Furthermore, the effects of the mechanical activation of SrTiO<sub>3</sub> powder on the occurrence of polar nano and micro-regions at room temperature, as well as the simultaneous influence of activation and MnO<sub>2</sub> addition on structural changes in ceramic SrTiO<sub>3</sub> samples, have also been analysed using Raman spectroscopy.

**Index Terms** — Raman spectroscopy, mechanical activation, BaTiO<sub>3</sub>, SrTiO<sub>3</sub>, nanocomposites, multiferroics.

## I. INTRODUCTION

Raman spectroscopy is primarily a vibrational spectroscopic method, used for non-destructive characterization of materials. It provides information on the vibrational spectra of molecules, which can be used to identify

certain compounds, crystal modifications or functional groups, as well as to trace some structural changes [1, 2]. The method is often considered to be complementary to IR spectroscopy and is widely used as an additional investigation procedure to XRD and other structural analyses. The principle of Raman spectroscopy relies on the inelastic scattering of monochromatic light on the crystal lattice of the investigated sample. The term *Raman spectroscopy* primarily refers to the scattering of photons by phonons [3]. The so-called Raman shift, which is the difference in the wave number of incident and scattered radiation, is the main parameter analyzed in Raman spectroscopy, because this difference directly depends on the type of molecules, molecular groups and certain crystal modifications, as well as in general on the structure of the tested sample.

BaTiO<sub>3</sub> and SrTiO<sub>3</sub> belong to the group of alkaline earth metal titanates usually considered to be model perovskite materials, i.e. easily functionalizable materials that are intensively and widely applied in electronics. Barium titanate has been the most extensively investigated lead-free ferroelectric material, with a high dielectric constant, widely utilized to manufacture electronic components. Most applications of barium titanate-based materials include the production of multilayer capacitors (MLCs), piezoelectric devices, positive temperature coefficient thermistors, high-density optical data storage, communication filters and nonvolatile memories, etc. [4]. Along with being used as sensors and multilayer ceramic capacitors (MLCCs), materials based on strontium titanate are also used as catalysis, in UV detectors and solar cells, in DRAMs and energy storage devices, etc. [5]. Due to the persisting need to miniaturize electronic devices, it is necessary to obtain smaller and more uniform particle sizes of electronic materials. Among numerous methods for the production of BaTiO<sub>3</sub> and SrTiO<sub>3</sub> fine powders, such as the sol-gel synthesis, oxalate process, hydrothermal synthesis, the combustion of a dehydrated form of the precursor complex, polymeric precursor and solvothermal methods, etc., mechanical activation has been identified as a very effective and low-cost method for obtaining a highly dispersed system, enabling the directed modification of the structure and properties of activated material. Barium titanate ceramics obtained from mechanically activated powders may have a higher piezoelectric coefficient, as well as modified values of

Vera P. Pavlović is with the University of Belgrade, Faculty of Mechanical Engineering, Kraljice Marije 16, 11120 Belgrade, Serbia (e-mail: vpavlovic@mas.bg.ac.rs).

Ani Tshantshapanyan is with the North Carolina Central University, 18001 Fayetteville Street, Durham, NC 27707, USA (e-mail: atshants@ncsu.edu)

Branislav Vlahović is with the North Carolina Central University, 18001 Fayetteville Street, Durham, NC 27707, USA (e-mail: vlahovic@ncsu.edu).

Jelena Živojinović is with the Institute of Technical Sciences of the Serbian Academy of Sciences and Arts, Knez Mihailova 35, 11000 Belgrade, Serbia (e-mail: jelena.zivojinovic@itn.sanu.ac.rs)

Darko Kosanović is with the Institute of Technical Sciences of the Serbian Academy of Sciences and Arts, Knez Mihailova 35, 11000 Belgrade, Serbia (e-mail: darko.kosanovic@itn.sanu.ac.rs)

Vladimir B. Pavlović is with the Institute of Technical Sciences of the Serbian Academy of Sciences and Arts, Knez Mihailova 35, 11000 Belgrade, Serbia (e-mail: vladimir.pavlovic@itn.sanu.ac.rs).

dielectric permittivity, a lower Curie point and a flattened curve of  $\epsilon_r = f(T)$  dependence, which are the effects analogue to those obtained by adding various additives such as SrTiO<sub>3</sub>, BaZrO<sub>3</sub> and SnTiO<sub>3</sub>, or CaTiO<sub>3</sub> and MgTiO<sub>3</sub> [6]. On the other hand, the mechanical activation of SrTiO<sub>3</sub> may influence not only its dielectric properties, but also its optical properties and electrical conductivity, regarding the increase in the concentration of defects such as oxygen vacancies.

The utilization of BaTiO<sub>3</sub> and SrTiO<sub>3</sub> materials as fillers within a polymer matrix in the production of composite materials with improved electroactive properties is also an increasingly interesting topic. Among the various polymers that can be used for these purposes, PVDF has been identified as a semi-crystalline fluoro-polymer which has polar crystalline phases, such as beta and gamma crystal modifications, along with non-polar ones. The ferroelectric and piezoelectric properties of PVDF are determined by the presence of these polar phases, especially the beta phase. It is noteworthy that PVDF, as well as the composites based on it, has some advantages over purely ceramic ferroelectric samples, since PVDF is marked by low density, high flexibility, sufficient strength, toughness and the ability to be easily produced in a technologically useful form [7]. It is generally recognized that PVDF and its co-polymers have a huge potential as dielectric materials, especially in those applications where high-energy density and low loss at high repetition rates are required [8].

It has been found that BaTiO<sub>3</sub>-based materials can simultaneously exhibit ferroelectricity and ferromagnetism at room temperature, depending on the type and concentration of the dopant. According to the literature data, the incorporation of 3d and 4d transition metals as a substitute for the titanium atom in barium titanate may produce ferromagnetism, inducing multiferroicity. For instance, room-temperature ferromagnetism has been reported in Mn-, Fe- and Co-doped BaTiO<sub>3</sub> systems. It has been observed that the substitution of Fe at the B-site improves the coercive field, while the substitution at the A-site increases saturation magnetization [9]. Besides, barium hexaferrite BaFe<sub>12</sub>O<sub>19</sub> (often denoted as BaM) and Fe-ion substituted ferrite materials based on it have been extensively used due to their multiferroic properties. Barium hexaferrite belongs to the M-type hexaferrites, which are based on a hexagonal "magnetoplumbite" or M-structure. This symmetry belongs to the space group P6<sub>3</sub>/mmc with 64 atoms in a unit cell [10]. BaM is marked by large spontaneous polarization at room temperature, a clear ferroelectric hysteresis loop, high saturation magnetization, high intrinsic coercivity (for both ferroelectric and magnetic hysteresis) and high ferrimagnetic transition temperature. These features make it suitable for application, especially if we keep in mind that it is possible to control both polarization and magnetization via an external electric and/or magnetic field [11]. The large uniaxial anisotropy can be overcome by substituting a Fe<sup>3+</sup> ion (e.g. with Co<sup>2+</sup> and Ti<sup>4+</sup>), which endows ferrite with an excellent soft magnetic property with a high magnetic permeability [12]. BaM has found wide applications in technology as a permanent magnet, in

microwave devices, sensors, particulate perpendicular high-density recording media, high-frequency circuits and in many other magnetically operated devices [10]. However, the production of pure or substituted BaM is normally accompanied with the presence of residual nonmagnetic phases, such as hematite ( $\alpha$ -Fe<sub>2</sub>O<sub>3</sub>), which can be associated with the choice of the Fe:Ba molar ratio in the starting powder. Therefore, an extensive research has been carried out to synthesize M-type hexaferrites from starting powders with an off-stoichiometric Fe:Ba ratio.

Doping SrTiO<sub>3</sub> with transition metals such as Mn is also interesting, not only with the aim of introducing ferromagnetic behavior and the coexistence of a glassy magnetic state and a glassy dielectric behavior in a Mn-doped SrTiO<sub>3</sub> system, but also to modify and tune dielectric permittivity and dielectric loss, which depends on the site of ion incorporation in the lattice (at the Sr or Ti site) [13]. To the best of our knowledge, there are no reports on the simultaneous effect of Mn-doping and mechanical activation of strontium titanate on its structure and properties.

This paper presents an overview of the application of nonresonant Raman spectroscopy in the analysis of structural changes in materials obtained from mechanically activated BaTiO<sub>3</sub> and SrTiO<sub>3</sub> powders. Having in mind the importance of obtaining light, flexible and easily processed electroactive nanocomposite films for the application in the production of pressure and IR sensors etc., structural changes in polymer composite films with a mechanically activated titanate as a filler were also analyzed using Raman spectroscopy. The Raman analysis of a mechanically activated Fe/BaTiO<sub>3</sub> system and hexaferrite BaTi<sub>x</sub>Fe<sub>12-x</sub>O<sub>19</sub> synthesized from this system is presented as well, including the investigation of the influence of laser power on the obtained results. The application of Raman spectroscopy in the assessment of the dopant incorporation into the SrTiO<sub>3</sub> lattice was additionally considered.

## II. MATERIALS AND METHODS

Commercially available BaTiO<sub>3</sub> powder (Aldrich, p.a. 99.9%) was mechanically activated in a planetary ball mill (Fritsch Pulverisette), up to 60 minutes, and an analogue procedure was applied for SrTiO<sub>3</sub> (99% purity, mean particle size  $\leq 5 \mu\text{m}$ ). The X-ray powder diffraction patterns of the initial and activated powders were obtained using CuK <sub>$\alpha$ 1/2</sub> filtered radiation. The Raman scattering of the samples was recorded at room temperature, in a backscattering geometry, using the 514.5 nm line of an Ar<sup>+</sup> ion laser for the BaTiO<sub>3</sub> spectra, and the 633 nm line of a He-Ne laser for the SrTiO<sub>3</sub> spectra. The BaTiO<sub>3</sub> that had been mechanically activated for a short period of time was used as a filler in the PVDF (polyvinylidene fluoride) matrix. The Raman spectra of these systems were taken by applying a He-Ne laser. Nanocomposite films were prepared by the solution casting method. In order to obtain the Sr<sub>1-x</sub>Mn<sub>x</sub>TiO<sub>3</sub> or SrTi<sub>1-x</sub>Mn<sub>x</sub>O<sub>3</sub> system, where  $x=0.03$ ,  $x=0.06$  and  $x=0.12$ , MnO<sub>2</sub> was added to the starting SrTiO<sub>3</sub> powder. The powders were

mechanically activated for 10, 30 and 120 min, under the same conditions as for pure SrTiO<sub>3</sub>, but with the addition of ethanol. After the activation, the samples were dried at 100 °C for 3.5 h and sintered at 1200 °C. The Raman examination of the influence of mechanical activation and doping was performed using the 532 nm line of the Nd:YAG laser. The mixture of commercially available Fe and BaTiO<sub>3</sub> powders (weight % ratio: 60:40) was also mechanically activated up to 240 minutes in a planetary ball mill, calcined at 700 °C for 2 h and sintered at 1200 °C, in order to obtain hexaferrite ceramics. The influence of mechanical activation on the Raman spectra of the calcined mixture and sintered samples was monitored using the 633 nm line of a He-Ne laser. Two different laser beam power values were applied on the sample.

### III. MAIN RESULTS

#### A. Raman spectra of mechanically activated barium titanate

The role of Raman spectroscopy in the assessment of the dominant crystal modification and in the monitoring of the trend of structural changes in mechanically activated BaTiO<sub>3</sub> was analysed as the first example. It is known that size effects can influence the stability of the BaTiO<sub>3</sub> ferroelectric phase at room temperature, leading to the occurrence of the cubic phase [14]. The critical size below which the BaTiO<sub>3</sub> crystal structure changes from the tetragonal (ferroelectric) to the cubic phase usually varies from 20 to 100 nm, depending on the processing route [15]. Mechanical activation can generally lead to significantly reduced mean particle and crystallite sizes, which is usually accompanied with an increased value of microstrains. The formation of uncompensated stress during mechanical activation also causes tetragonal distortion, which can be manifested as the change in crystal lattice parameters [16, 17]. All these effects cause both the broadening of diffraction lines and the decrease in their integral intensity, making the assessment of the crystal structure type much more difficult (Fig. 1).

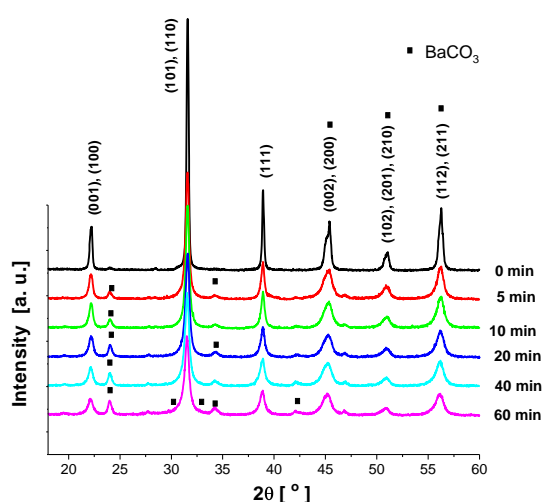


Fig. 1. XRD spectra of mechanically activated barium titanate.

Generally, the XRD peak in the range  $2\theta \in (44 - 46)^\circ$  is especially important in estimating the presence of the cubic or tetragonal crystal modification of BaTiO<sub>3</sub>. Namely, in a typical tetragonal structure with micron-sized crystallites, the mentioned peak occurs as a doublet (002, 200), with a clearly expressed split of the peak into two components. On the other hand, in a typical cubic structure there is no splitting and the peak is completely symmetrical. However, in case of a slightly sustained tetragonal or pseudocubic structure in BaTiO<sub>3</sub>, where the mean crystallite size is on the scale of 100 nm or less, only the weak peak asymmetry instead of splitting may be observed, due to the broadening, shifting and overlapping of diffraction lines [14]. Therefore, in fine-grained and nanocrystalline BaTiO<sub>3</sub> careful additional comparison between the widths of the doublet and a singlet is required, as well as a very careful Rietveld refinement of the whole diffractogram. In such cases, it is especially important to obtain information about the present crystal modifications on the basis of other nondestructive methods, such as Raman spectroscopy. Although the tetragonal BaTiO<sub>3</sub> has eight Raman active modes (three A<sub>1</sub>, one B<sub>1</sub> and four E modes) according to theoretical selection rules, the effects like the overlapping of some modes (A<sub>1</sub> and E, or B<sub>1</sub> and E) and the existence of a coupled-mode interaction, as well as the overdamped character of the lowest optical E mode (E(1TO) soft mode), commonly lead to a smaller number of Raman peaks in the experimentally obtained unpolarized spectrum of polycrystalline samples. It can be seen in Fig. 2 that all experimentally expected Raman peaks, typical for microcrystalline BaTiO<sub>3</sub> powders and ceramics [18,19], are found in the spectrum of the nonactivated sample.

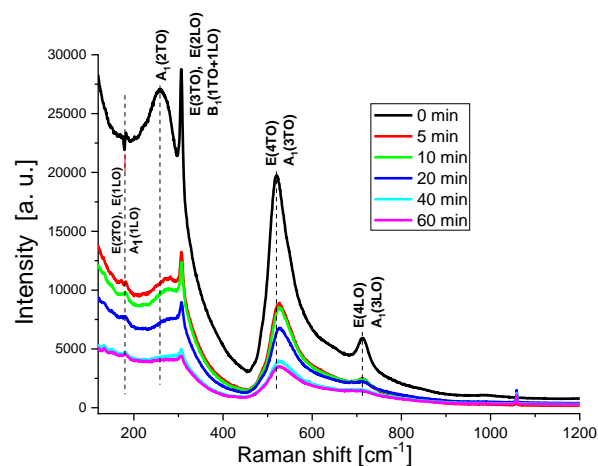


Fig. 2. Raman spectra of mechanically activated barium titanate.

It is demonstrated that a diminution in particle and crystallite size during mechanical activation lasting up to 60 minutes, as well as an increased concentration of defects and the disorder induced in the BaTiO<sub>3</sub> powders activated for longer periods, lead to decreased peak intensities, accompanied with their gradual broadening. The sharpest peak, known as typical of the tetragonal BaTiO<sub>3</sub> structure, decreases as well in the

obtained spectra, but remains sufficiently noticeable even for prolonged activation times, indicating possible domination of the tetragonal structure in the nanocrystalline powder, although with a slightly sustained tetragonality. This example illustrates the importance of Raman spectroscopy application in assessing the presence of the tetragonal crystal modification in the perovskite structure, especially when particle and crystallite sizes in the material are sufficiently small to cause a prominent broadening and the overlapping of the XRD lines essential for the polymorph phase discrimination. The conclusions derived based on Raman spectroscopy may be very helpful in the Rietveld analysis of XRD spectra. In this case, the Rietveld analysis of the X-ray diffraction patterns of mechanically activated  $\text{BaTiO}_3$ , correlated with the observations from the Raman spectra, shows that mechanical activation for up to 60 minutes lead to a significant reduction of the mean crystallite size from 150 nm to  $\sim 30$  nm [20], but the tetragonal structure persist as the dominant. The deconvolution of the Raman spectra may reveal important parameters, such as the positions of the modes and the relative change of the FWHM values (Fig. 3).

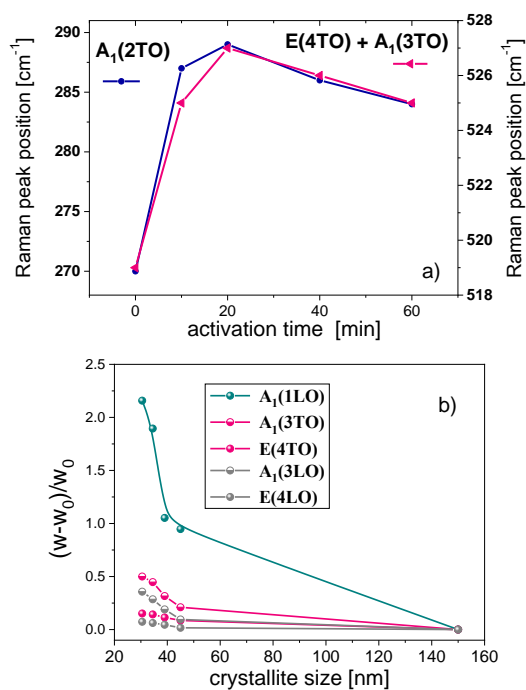


Fig. 3. a) The influence of activation time on the position of those Raman peaks which include  $A_1(\text{TO})$  modes; b) Relative change of the FWHM for modes assigned to Raman peaks at  $\sim 180$ ,  $520$  and  $720 \text{ cm}^{-1}$ , versus crystallite size.

In case of mechanically activated  $\text{BaTiO}_3$ , the significant blue shift of the two main broad Raman peaks observed in the range up to  $600 \text{ cm}^{-1}$  (Fig. 3a) confirms that the  $A_1(\text{TO})$  modes are sensitive to impurities or structural defects, although the mentioned shift could also be attributed to mechanically introduced stress effects, primarily to an increased tensile stress [21]. Some of the low-intensity bands in the region under  $170 \text{ cm}^{-1}$  are detected in the samples

activated for longer periods (Fig. 2), indicating changes in the vibrations of Ti and  $\text{TiO}_6$  octahedra, due to the formation of oxygen and/or barium vacancies and other  $\text{BaTiO}_3$  intrinsic structural defects [22].

### B. Raman spectra of PVDF polymer and PVDF-based nanocrystalline composites

Raman spectroscopy was also applied for the assessment of the type of the dominant crystal modification of the low-density fluoro-polymer PVDF matrix, after the incorporation of mechanically activated  $\text{BaTiO}_3$  as a filler [23]. It is known that PVDF is a semi-crystalline fluoro-polymer, which can crystallize in several modifications. Although theoretically five crystal modifications may occur, some of the following three phases are usually present: alpha, beta and gamma. The alpha phase is the most common, but electroactive phases such as beta and gamma are important for application in electrical components. Only the  $\beta$ -phase is suitable for most sensor applications, since it has the most pronounced ferro-, piezo- and pyroelectric properties, due to larger spontaneous polarization [24, 25]. For these reasons, intensive research efforts towards obtaining PVDF films with the largest possible share of the beta phase are of key interest. Since some of the strongest XRD lines of the three common PVDF crystal phases ( $\alpha$ ,  $\beta$  and  $\gamma$ ) are very close to each other and they partially overlap, the investigation of Raman spectra may be crucial for the conclusions regarding the present phases. The broad-ranged Raman spectra of polymers are very complex to analyze, not only due to the multitude of peaks belonging to the polymer and the filler, but also because of the frequent emergence of fluorescence, which raises the background signal, thereby reducing the observable intensity of the diffraction lines belonging to crystal phases. The part of the entire recorded Raman spectrum of the PVDF-based composites that is the most relevant for the identification of crystalline phases in the PVDF polymer and the PVDF-based composites is presented in Fig. 4.

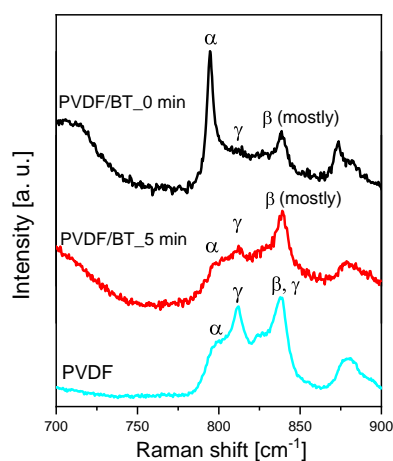


Fig. 4. The enlarged part of Raman spectra of PVDF and PVDF-based composites with non-activated and activated  $\text{BaTiO}_3$  as a filler.

Fig. 4 shows how the incorporation of the nonactivated and shortly activated  $\text{BaTiO}_3$  powder into the PVDF matrix changes the share of crystalline phases in the polymer, i.e. in the composite. It can be observed that the gamma phase dominates in the analyzed pure PVDF polymer, because the peak at  $812\text{ cm}^{-1}$  is clearly expressed only when the gamma phase is dominant [26]. The injection of the nonactivated  $\text{BaTiO}_3$  powder, with a weight fraction of 2%, enhances the domination of the alpha phase, while the injection of the same amount of the  $\text{BaTiO}_3$  powder activated for 5 minutes promotes the formation of the beta phase, which becomes dominant. This was probably caused by the smaller particle sizes, a larger specific surface area and consequently higher surface activity of the mechanically activated powder. Namely, these modifications were detected in the  $\text{BaTiO}_3$  powder activated for a short period using SEM method and mercury porosity [27]. Such modifications of the filler particles may amplify the interaction between the filler and the polymer, promoting the conformation of the polymer chains corresponding to the beta crystalline phase of PVDF. The share of the beta phase in the activated filler is significantly larger than the share of the gamma phase, while the formation of the alpha phase is suppressed. This is an important effect, since the beta phase of PVDF has the most pronounced ferroelectric properties, while the nanocrystalline filler activated for a short period keeps the tetragonal (ferroelectric) structure almost unchanged.

### C. Raman spectra of Fe/BaTiO<sub>3</sub> system and hexaferrite

In the previous sections, the examples of Raman analyses of a one-component system ( $\text{BaTiO}_3$  powder) and a two-component PVDF/BT system were discussed. In the latter case we can even speak of a multi-component system, if we consider the number of the crystalline modifications of PVDF. Having in mind the increasing importance of the development of multiferroic materials, we will present the application of Raman analyses for the examination of the mechanically activated Fe/BaTiO<sub>3</sub> system and the subsequent hexaferrite formation during the sintering process, in the following passages. A mixture of Fe and  $\text{BaTiO}_3$  powders (weight percent ratio: 60:40) was mechanically activated up to 240 minutes in a planetary ball mill and calcined at  $700\text{ }^\circ\text{C}$  for 2 h. The phase composition was investigated by means of the XRD and Raman methods. Since Raman spectroscopy cannot be used to detect pure metal modes, there are no modes in the Raman spectrum that corresponded to iron, while the diffraction patterns show distinct Fe peaks for all activation times [28]. The dependency of the obtained Raman spectra on both time of mechanical activation and the laser beam power at the sample was studied. The Raman spectra recorded under the lower power at the sample ( $0.6\text{ mW}$ ) show that the mechanical activation longer than 100 minutes promotes the formation of hematite during the activation and leads to the formation of other iron-oxide phases, such as magnetite and wustite (Fig. 5). The Raman spectrum of the sample corresponding to the longest activation time reveals the domination of iron oxide. The hematite mode corresponding

to the second order scattering also appears. These results are completely consistent with the obtained XRD spectrum [28]. After correlating the lower- and higher-power Raman spectra with the XRD results, it has been concluded that the increase in the beam power at the sample up to  $1.2\text{ mW}$  changes the phase ratio in the sample, i.e. causes an enhanced phase transition from magnetite to hematite (Fig. 6).

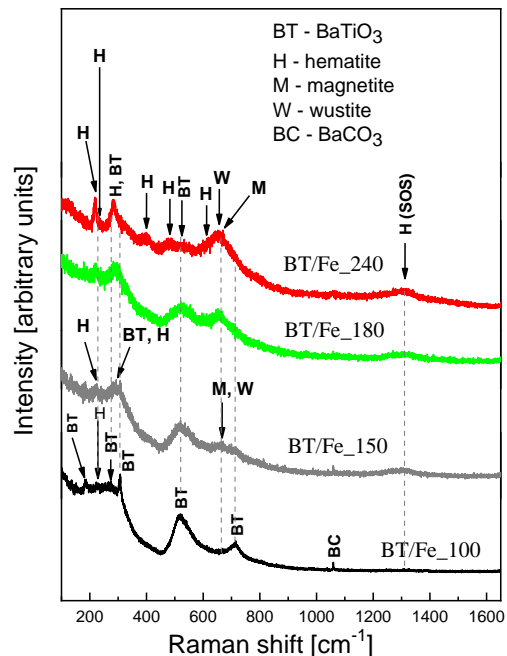


Fig. 5. Raman spectra of mechanically activated mixture of Fe and  $\text{BaTiO}_3$  powders (the power of a laser beam at the sample:  $0.6\text{ mW}$ ).

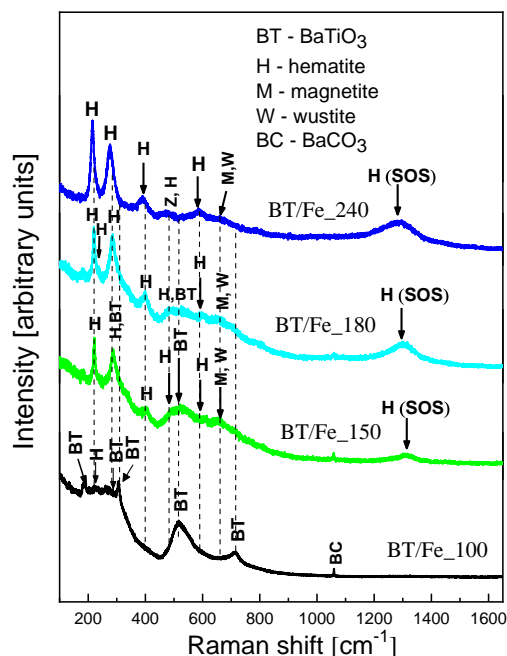


Fig. 6. Raman spectra of mechanically activated mixture of Fe and  $\text{BaTiO}_3$  powders (the power of a laser beam at the sample:  $1.2\text{ mW}$ ).

It has also been observed that mechanical activation decreases the temperature of the phase transition from wustite to magnetite and from magnetite to hematite. This effect emphasizes that in Raman spectroscopy the laser power on the sample does not only affect the signal strength, but can cause a local increase in temperature that is sufficient to give rise to some phase transitions in certain systems such as iron oxide, thus significantly changing the spectrum. Although our higher laser power value was still in the range where no phase transition from one iron-oxide phase to another was expected in the nonactivated sample, mechanical activation changed the upper limit of the mentioned range. Based on the literature data about the influence of laser power on phase transition in nonactivated magnetite [29], we can conclude that the transition from magnetite to hematite takes place at a much lower power in the mechanically activated samples, than in nonactivated magnetite.

The calcined samples were sintered at 1200 °C, in order to obtain hexaferrite. The Raman spectra of the sintered samples are shown in Fig. 7. Both XRD and Raman analyses indisputably show that hexaferrite (pure or cation-substituted) was formed in all samples (for all activation times) and that hexaferrite modes were dominant [30].

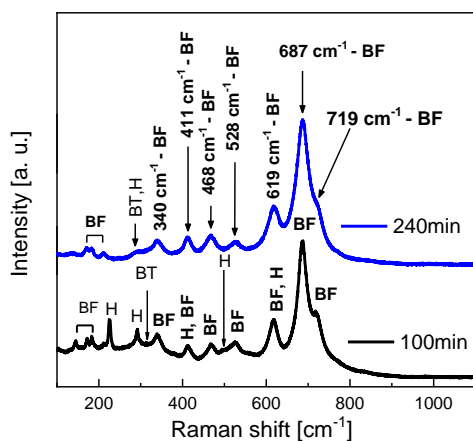


Fig. 7. Raman spectra of ceramics obtained from mechanically activated Fe/BaTiO<sub>3</sub> system (BF – barium hexaferrite, BT – BaTiO<sub>3</sub>, H – hematite).

Weak modes of residual hematite and BaTiO<sub>3</sub> are also observed in the spectrum. The number and intensity of these modes decrease with prolonged mechanical activation, as expected. However, it should be noticed that the Raman spectra presented in Fig. 7 do not indicate an unambiguous conclusion regarding the formula of hexaferrite. The XRD analysis suggests that Ti-substituted BaM was obtained, i.e. BaTi<sub>x</sub>Fe<sub>12-x</sub>O<sub>19</sub>, which could be expected based on the starting components. Namely, the Ritveld analysis (the refinement of the entire diffraction profile, the determination of the occupation numbers, etc.), indicates that the formula of the obtained hexaferrite is: BaFe<sub>11.23</sub>O<sub>19</sub>Ti<sub>0.77</sub>. Yet, according to the literature data [10, 31] our Raman spectra have the characteristics of both compounds – pure BaM and Ti-substituted hexaferrite, which makes an estimation of the

parameter  $x$  more difficult. The reason for the highlighted ambiguity lies in the fact that barium hexaferrite belongs to very complex systems. It has 64 ions per unit cell, on 11 different symmetry sites, where 24 Fe<sup>3+</sup> ions are distributed over five different symmetry sites: three kinds of octahedral sites, one tetrahedral site and one bipyramidal site [10]. Although Raman spectroscopy can be used to study the distribution of cations in a system, the assessment is usually sufficiently accurate in less complicated systems. In addition, despite the widespread application of the BaM system, it is still impossible to find a sufficiently complete database for its Raman spectra, and the existing spectra of BaM and Ti-substituted BaM sometimes seem contradictory, both in terms of peak shapes and peak positions. Therefore, it is of great interest to enrich the existing databases with the Raman spectra of pure and cation-substituted barium hexaferrite obtained via different procedures.

#### D. Raman spectra of mechanically activated undoped and Mn-doped SrTiO<sub>3</sub>

The analysis of the Raman spectra of the mechanically activated SrTiO<sub>3</sub> reveals that along with the dominant second-order scattering several very weak first-order Raman modes occur (Fig. 8) due to imperfections in the SrTiO<sub>3</sub> cubic structure at room temperature. While the intensity of second-order peaks decreases with the longer activation times, the intensity of the polar modes TO<sub>2</sub> and TO<sub>4</sub> increases. The modes X<sub>1</sub> and X<sub>2</sub> show similar dependence. According to the literature data, the shape and the intensity of polar TO modes in SrTiO<sub>3</sub> may significantly depend on defects such as oxygen vacancies [32].

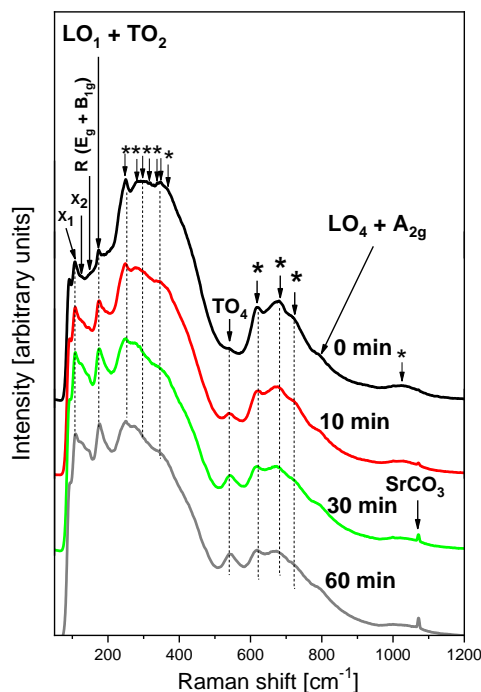


Fig. 8. Raman spectra of mechanically activated strontium titanate.

The characteristic Fano shape of the  $\text{TO}_2$  Raman line suggests a high probability of the presence of polar micro- and nanoregions (which coexist with the dominant paraelectric phase) in the activated  $\text{SrTiO}_3$ . A considerable increase in the  $\text{TO}_4$  mode intensity (Fig. 8) supports this assumption as well. It is accepted in the literature that the  $\text{TO}_2$  mode intensity is proportional to the total volume of polar microregions, and that the occurrence of  $\text{TO}_2$  mode may be accompanied with the remnant polarization [33]. However, the silent mode remains unnoticeable in the activated samples, indicating that the long-range structural distortion has not been established, as well as that the number of polar micro-regions is small and there is still no overlap between the adjacent polar micro-regions. The performed Raman spectroscopy gives clear evidence about the blue shift of the  $\text{TO}_4$  mode,  $\text{X}_1$  mode and ( $\text{LO}_1+\text{TO}_2$ ) doublet (Fig. 8), which is primarily a result of the introduction of microstress into the  $\text{SrTiO}_3$  lattice, but also a consequence of the reduced crystallite sizes.

Additional investigations were performed in order to apply Raman spectroscopy for monitoring the influence of mechanical activation on incorporation of the Mn ions into the  $\text{SrTiO}_3$  lattice. In order to obtain a  $\text{Sr}_{1-x}\text{Mn}_x\text{TiO}_3$  or  $\text{SrTi}_{1-x}\text{Mn}_x\text{O}_3$  system, where  $x=0.03$ ,  $x=0.06$  and  $x=0.12$ ,  $\text{MnO}_2$  was added to the starting  $\text{SrTiO}_3$  powder. The powders were mechanically activated for 10, 30 and 120 minutes, under the same conditions as for a pure  $\text{SrTiO}_3$ , but with the addition of ethanol. After activation, the samples were dried at  $100^\circ\text{C}$  for 3.5 h and sintered at  $1200^\circ\text{C}$ . The spectra of the nonactivated samples and of the samples activated for 120 min are shown in Fig. 9, which includes undoped and differently doped samples.

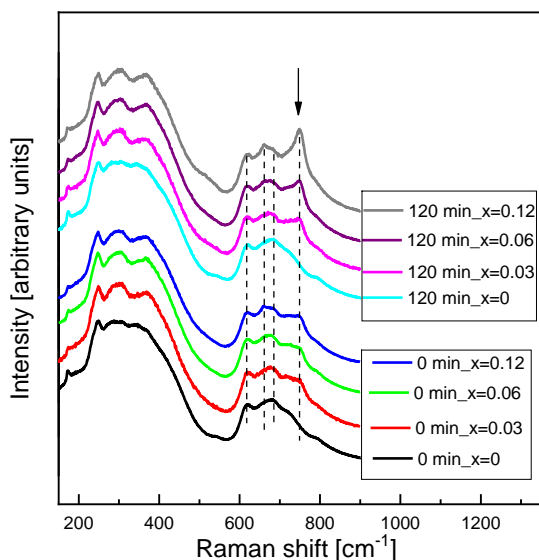


Fig. 9. Raman spectra of Mn-doped  $\text{SrTiO}_3$  ceramics.

Fig. 9 shows that the peaks obtained as a result of the second order scattering are generally more distinct in doped samples, especially in the Raman shift range above  $720\text{ cm}^{-1}$ . Actually, in those samples the occurrence of the peak at  $\sim 750\text{ cm}^{-1}$  is

observed, whereby its intensity increases with increased dopant concentration. The influence of the changes in the manganese concentration on the high-frequency part of the broad second-order Raman effect in the Raman shift region above  $590\text{ cm}^{-1}$ , in the  $\text{Sr}_{1-x}\text{Mn}_x\text{TiO}_3$  and  $\text{SrTi}_{1-x}\text{Mn}_x\text{O}_3$  systems has also been observed by K.R.S. Preethi Meher et al. and V. Trepakov et al. [34, 35]. According to the literature data, the position of the mentioned peak at  $\sim 750\text{ cm}^{-1}$  does not correspond to the position of any of the stronger modes of manganese oxide ( $\text{MnO}$ ,  $\text{MnO}_2$  or  $\text{Mn}_3\text{O}_4$ ) and does not correspond to pure  $\text{SrTiO}_3$  [36, 37]. This peak is not present in the spectrum of  $\text{Mn}_3\text{O}_4$  and is barely noticeable in the spectra of some crystalline modifications of  $\text{MnO}_2$ . Since the peak at  $\sim 750\text{ cm}^{-1}$  is clearly visible in the spectra of doped samples, where its intensity increases with increasing dopant concentration and this is not accompanied with the occurrence or increased intensity of any of the two strongest  $\text{MnO}_2$  modes, it may be concluded that the observed change in the intensity of this peak with the increasing value of  $x$  indicates the incorporation of Mn ions into the  $\text{SrTiO}_3$  lattice.

As it can be seen from Fig. 9, the application of mechanical activation leads to a more pronounced increase in the intensity of the peak at  $\sim 750\text{ cm}^{-1}$ , indicating that the activation causes an effectively higher incorporation of the dopant into the strontium-titanate lattice.

#### IV. CONCLUSION

In summary, this paper offers an important overview of the role and the advantages of nonresonant Raman spectroscopy, which is presented using the examples that illustrate the analyses of structural changes in electronic materials obtained from mechanically activated  $\text{BaTiO}_3$  and  $\text{SrTiO}_3$  powders. The doping effect, the obtaining of nanocomposites with an enhanced share of the electroactive crystalline phase of a polymer matrix and the obtaining of hexaferrite as a multiferroic material are considered in the paper, as well. The influence of the laser beam power on the spectra is also discussed.

#### ACKNOWLEDGMENT

This work was supported by the Ministry of Education, Science and Technological Development of the Republic of Serbia under the contracts 451-03-68/2020-14/200105 and NSF-RISE 1829245, NSF-PREM 1523617, and NSF CREST 1345219 awards.

#### REFERENCES

- [1] D. J. Gardiner, P. R. Graves (Editors); with contributions by H. J. Bowley [and five others], *Practical Raman Spectroscopy*, Berlin, Germany: Springer-Verlag, 1989.
- [2] B. Schrader, *Infrared and Raman Spectroscopy - Methods and Applications*, Weinheim, Germany: VCH, 1995
- [3] R. Merlin, A. Pinczuk, W. H. Weber, *Overview of Phonon Raman Scattering in Solids*, Chapter in *Raman Scattering in Materials Science*, Springer Series in Materials Science, book series vol. 42, pp. 1-29, Springer, Berlin, Heidelberg, Germany: Springer, 2000.
- [4] B. Ertuğ, "The overview of the electrical properties of barium titanate", *Am. J. Eng. Res.*, vol. 2, no. 8, pp. 01-07, 2013.

- [5] E Guo, L Yin, "Tailored SrTiO<sub>3</sub>/TiO<sub>2</sub> heterostructures for dye-sensitized solar cells with enhanced photoelectric conversion performance", *J. Mater. Chem. A*, vol. 3, no. 25, pp. 13390-13401, May 2015.
- [6] J. H. Jeon, Y. D. Hahn, H. D. Kim, "Microstructure and dielectric properties of barium-strontium titanate with a functionally graded structure", *J. Eur. Ceram. Soc.*, vol. 21, no. 10-11, pp. 1653-1656, August 2001.
- [7] X. Qiu, "Patterned piezo-, pyro- and ferroelectricity of poled polymer electrets", *J. Appl. Phys.*, vol. 108, no. 1, pp. 011101, July 2010.
- [8] V. Tomer, E. Manias, C.A. Randal, "High field properties and energy storage in nanocomposite dielectrics of poly(vinylidene fluoride-hexafluoropropylene)", *J. Appl. Phys.*, vol. 110, no. 4, pp. 044107, August 2011.
- [9] A. Rani, J. Kolte, S. S. Vadla, P. Gopalan, "Structural, Electrical, Magnetic and Magnetoelectric properties of Fe doped BaTiO<sub>3</sub> ceramics", *Ceram. Int.*, vol. 42, no. 7, pp. 8010-8016, May 2016.
- [10] F. M. Silva Junior, C. W. A. Paschoal, "Spin-phonon coupling in BaFe<sub>12</sub>O<sub>19</sub> M-type hexaferrite", *J. Appl. Phys.*, vol. 116, no. 24, pp. 244110, December 2014.
- [11] G. Tan, X. Chen, "Structure and multiferroic properties of barium hexaferrite ceramics", *Journal of Magnetism and Magnetic Materials*, vol. 327, pp. 87-90, February 2013.
- [12] J. Li, H. Zhang, Y. Liu, Q. Li, H. Zhou, H. Yang, "Phase formation, magnetic properties and Raman spectra of Co-Ti co-substitution M-type barium ferrites", *Appl. Phys. A*, vol. 119, no. 2, pp. 525-532, January 2015.
- [13] D. Choudhury, S. Mukherjee, P. Mandal, A. Sundaresan, U. V. Waghmare, S. Bhattacharjee, R. Mathieu, P. Lazor, O. Eriksson, B. Sanyal, P. Nordblad, A. Sharma, S. V. Bhat, O. Karis, D. D. Sarma, "Tuning of dielectric properties and magnetism of SrTiO<sub>3</sub> by site-specific doping of Mn", *Phys. Rev. B*, vol. 84, no. 12-15, pp. 125124, September 2011.
- [14] T. Yan, Z. G. Shen, W. W. Zhang, J. F. Chen, "Size dependence on the ferroelectric transition of nanosized BaTiO<sub>3</sub> particles", *Mater. Chem. Phys.*, vol. 98, no. 2-3, pp. 450-455, August 2006.
- [15] Y. I. Kim, J. K. Jung, and K. S. Ryu, "Structural Study of Nano BaTiO<sub>3</sub> Powder by Rietveld Refinement", *Mater. Res. Bull.*, vol. 39, no. 7-8, pp. 1045-1053, June 2004.
- [16] W. Peukert, "Material properties in fine grinding", *Int. J. Miner. Process.*, vol. 74, Supplement, pp. S3-S17, December 2004.
- [17] V. P. Pavlović, B. Vlahović, D. Kosanović, M. Dukić, M. Wu, V. B. Pavlović, "Mechanically Activated Ferroelectric Materials", Proc. of 3rd International conference on Electrical, Electronic and Computing Engineering – IcETRAN 2016, Zlatibor, Serbia, pp. NMI1.1-8, June 13-16, 2016.
- [18] T. Hoshina, H. Kakemoto, T. Tsurumi, S. Wada, "Size and Temperature Induced Phase Transition Behaviors of Barium Titanate Nanoparticles", *J. Appl. Phys.*, vol. 99, no. 5, pp. 054311, March 2006.
- [19] R. Naik, J. J. Nazarko, C. S. Flattery, U. D. Venkateswaran, V. M. Naik, M. S. Mohammed, G. W. Auner, J. V. Mantese, N. W. Schubring, A. L. Micheli, and A. B. Catalan, "Temperature Dependence of the Raman Spectra of Polycrystalline Ba<sub>1-x</sub>Sr<sub>x</sub>TiO<sub>3</sub>", *Phys. Rev. B*, vol. 61, no. 17, pp. 11367-11372, May 2000.
- [20] V. P. Pavlović, M. V. Nikolic, V. B. Pavlović, J. Blanus, S. Stevanovic V. V. Mitic, M. Scepanovic, "Raman Responses in Mechanically Activated BaTiO<sub>3</sub>", *J. Am. Ceram. Soc.*, vol. 97, no. 2, pp. 601-608, January 2014.
- [21] B. Wang and L. Zhang, "Size Effects on Structure and Raman Spectra of BaTiO<sub>3</sub> Thin Film", *Phys. Status Solidi A*, vol.169, no.1, pp. 57-62, September 1998.
- [22] M. Zhang, J. Yu, J. Chu, Q. Chen, and W. Chen, "Microstructures and Photoluminescence of Barium Titanate Nanocrystals Synthesized by the Hydrothermal Process", *J. Mater. Process. Technol.*, vol. 137, no. 1-3, pp. 78-81, June 2003.
- [23] V. P. Pavlović, V. B. Pavlović, B. Vlahović, D. K. Božanić, J. D. Pajović, R. Dojčić and V. Djoković, "Structural properties of composites of polyvinylidene fluoride and mechanically activated BaTiO<sub>3</sub> particles", *Physica Scripta*, T157, pp. 014006-1-5, November 2013.
- [24] R. Gregorio, "Determination of the  $\alpha$ ,  $\beta$  and  $\gamma$  crystalline phases of poly(vinylidene fluoride) films prepared at different conditions", *J. Appl. Polym. Sci.*, vol. 100, no. 4, pp. 3272-3279, May 2006.
- [25] N. J. Ramer, T. Marrone, K. Stiso, "Structure and vibrational frequency determination for  $\alpha$ -poly (vinylidene fluoride) using density-functional theory", *Polymer*, vol. 47, no. 20, pp. 7160-7165, September 2006.
- [26] T. Boccaccio, A. Bottino, G. Capannelli, P. Piaggio, "Characterization of PVDF membranes by vibrational spectroscopy", *J. Membr. Sci.*, vol. 210, no. 2, pp. 315-329, December 2002.
- [27] V. P. Pavlović, D. Popović, J. Krstić, J. Dojčić, B. Babić, V. B. Pavlović, "Influence of Mechanical Activation on the Structure of Ultrafine BaTiO<sub>3</sub> Powders", *J. Alloys Compd.*, vol. 486, no. 1-2, pp. 633-639, July 2009.
- [28] D. Kosanović, N. Obradović, V. P. Pavlović, S. Marković, A. Maričić, G. Rasić, B. Vlahović, V. B. Pavlović, M. M. Ristić, "The influence of mechanical activation on the morphological changes of Fe/BaTiO<sub>3</sub> powder", *Materials Science and Engineering B: Advanced Functional Solid-State Materials*, vol. 212, pp. 89-95, October 2016.
- [29] D. L. A. de Faria, S. Venaúncio Silva, M. T. de Oliveira, "Raman microspectroscopy of some iron oxides and oxyhydroxides", *Journal of Raman Spectroscopy*, vol. 28, no. 11, pp. 873-878, November 1997.
- [30] D. Kosanović, V. A. Blagojević, A. Maričić, S. Aleksić, V. P. Pavlović, V.B. Pavlović, B. Vlahović, "Influence of mechanical activation on functional properties of barium hexaferrite ceramics", *Ceramics International*, vol. 44, no. 6, pp. 6666-6672, April 2018.
- [31] D. A. Vinnik, V. E. Zhivulin, A. Yu. Starikov, S. A. Gudkova, E. A. Trofimov, A. V. Trukhanov, S. V. Trukhanov, V. A. Turchenko, V. V. Matveev, E. Lahderanta, E. Fadeev, T. I. Zubar, M. V. Zdorovets, A. L. Kozlovsky, "Influence of titanium substitution on structure, magnetic and electric properties of barium hexaferrites BaFe<sub>12-x</sub>Ti<sub>x</sub>O<sub>19</sub>", *Journal of Magnetism and Magnetic Materials*, vol. 498, pp. 166117, March 2020.
- [32] J. Živojinović, V. P. Pavlović, D. Kosanović, S. Marković, J. Krstić, V. A. Blagojević, V. B. Pavlović, "The Influence of Mechanical Activation on Structural Evolution of Nanocrystalline SrTiO<sub>3</sub> Powders", *Journal of Alloys and Compounds*, vol. 695, pp. 863-870, February 2017.
- [33] Y. L. Du, G. Chen, M.S. Zhang, "Investigation of structural phase transition in polycrystalline SrTiO<sub>3</sub> thin films by Raman spectroscopy", *Solid State Communications*, vol. 130, no. 9, pp. 577-580, June 2004.
- [34] K. R. S. Preethi Meher, C. Bogicevic, P. E. Janolin, K. B. R. Varma, "Synthesis dependent characteristics of Sr<sub>1-x</sub>Mn<sub>x</sub>TiO<sub>3</sub> (x=0.03, 0.05, 0.07 and 0.09)", *J. Solid State Chem.*, vol. 192, pp. 296-304, August 2012.
- [35] V. Trepakov, M. Makarova, O. Stupakov, E. A. Tereshina, J. Drahokoupil, M. Cernanský, Z. Potucek, F. Borodavka, V. Valvoda, A. Lynnyk, A. Jäger, L. Jastrabik, A. Dejneka, "Synthesis, structure and properties of heavily Mn-doped perovskite-type SrTiO<sub>3</sub> nanoparticles", *Materials Chemistry and Physics*, vol. 143, no. 2, pp. 570-577, January 2014.
- [36] P. Y. Kuang, M. H. Liang, W. Y. Kong, Z. Q. Liu, Y. P. Guo, H. J. Wang, N. Li, Y. Z. Su, S. Chen, "Anion-assisted one-pot synthesis of 1D magnetic  $\alpha$ - and  $\beta$ -MnO<sub>2</sub> nanostructures for recyclable water treatment application", *New J. Chem.*, vol. 39, no. 4, pp. 2497-2505, January 2015.
- [37] B. J. Rani, M. Ravina, G. Ravi, S. Ravichandran, V. Ganesh, R. Yuvakkuma, "Synthesis and characterization of Hausmannite (Mn<sub>3</sub>O<sub>4</sub>) nanostructures", *Surfaces and Interfaces*, vol. 11, pp. 28-36, June 2018.